Wetting Effect on Torricelli's Law

J. Ferrand, L. Favreau, S. Joubaud, and E. Freyssingeas*

Université de Lyon, ENS de Lyon, Université Claude Bernard Lyon 1, CNRS, Laboratoire de Physique, F-69342 Lyon, France

(Received 5 July 2016; revised manuscript received 6 October 2016; published 7 December 2016)

This Letter presents an experimental study on the effect of wetting on the draining of a tank through an orifice set at its bottom. The investigation focuses on flows of liquids in the inertial regime through an orifice the size on the order of magnitude of the capillary length. The results show that although the flows always follow a Torricelli-like behavior, wetting strongly affects the speed of drainage. Surprisingly, this speed goes through a minimum as the outside surface of the tank bottom plate changes from hydrophilic to hydrophobic. The maximum effect in slowing down the flows (up to 20%) is obtained for a static wetting angle θ_s of about 60°. Experiments suggest that the effect of wetting on the exit flows, very likely, is related to the meniscus that forms at the hole's outlet. A simple model is proposed that estimates the variation of kinetic energy within the meniscus. This model captures the main features of the experimental observations, particularly the nonmonotonic variation of the speed of drainage as a function of θ_s with a minimum for a static wetting angle of about 60°.

DOI: 10.1103/PhysRevLett.117.248002

The draining of a tank through an orifice was first described by Torricelli almost 400 years ago [1]. In this model the energy losses are neglected (i.e., inviscid fluid), which led to the conclusion that the efflux velocity of the fluid v_T equals the velocity that the fluid would acquire if allowed to fall from the free surface of the reservoir to the opening. This results in the following equation: $v_T(t) = \sqrt{2gh(t)}$, where g is the acceleration due to gravity and $h(t)$ the height of fluid in the tank at time t. On that basis it is easy to obtain the expression for the drained volume versus time. This description has no free parameter; it only depends on the initial height of fluid, the tank geometry, and the hole's radius. Nevertheless, since it contains no dissipation, Torricelli's model always overestimates fluid velocity. Because this physical situation is a big issue in industry (agri-food, oil, etc.) as illustrated in a large amount of engineering books [2], many investigations have tried to correct this model [3–9]. All these corrections use empirical coefficients. For example, a proportionality coefficient α was introduced in Torricelli's equation, $v_T^{\mathrm{corr}}(t) = \alpha\sqrt{2gh(t)}$, to explain the difference between Torricelli's law and experimental observations [7]. Despite these efforts, the influence of some parameters is still not predictable. This is the case for the influence of wettability of the interfaces. Wetting has been studied extensively for many years [10,11]; however, its influence on macroscopic flows has not been investigated much so far [12–16]. To the best of our knowledge, no one has considered the effect of wetting on the tank draining. For example, what happens if the flowing fluid wets, or not, the surface surrounding the opening? One may expect a strong effect if the size of the hole is smaller or on the order of magnitude than the characteristic length scale that compares the respective effects of surface tension and gravity forces, namely, the capillary length; $\kappa^{-1} = \sqrt{\gamma/\rho g}$, where γ is the air-liquid surface tension of the fluid and ρ its density. In this latter case, one can imagine that the surface wettability (in other words the contact angle θ_s between the fluid and the outer surface) might monitor the flow rate.

The question we address in this Letter is the impact of wetting on Torricelli's model when the size of the opening is comparable to κ^{-1}. For that purpose, we built a specific experimental device that is described below, as well as the obtained results. We then propose a simple model to qualitatively explain the experimental observations.

Experimental setup (supplemental material, Appendix A).—The experimental device consists of a square tank ($a \times a$ with $a = 10$ cm) made of two Dural plates and two glass plates that is set down on a raised shelf. The bottom of the tank is a thin plate (2 mm) with a calibrated cylindrical hole of radius r_0 at its center. This plate is removable allowing us to change the size of the hole or the plate material. The fluid temperature within the tank is regulated to 25 ± 0.5 °C with 2 Peltier elements on both Dural plates. Using the shadowgraph technique, movies of the liquid jet at the exit of the tank during emptying are recorded at a constant frame rate (10–100 Hz) by means of a CCD camera (*Basler acA200–165 um*) and a macro lens (18–108 mm). An electronic scale accurate to 0.1 g (*KERN 532*) placed 20 cm below the tank measures the drained mass of liquid as a function of time at a sample rate of 5 Hz. The drained mass is then converted into drained volume using the fluid density.

Results shown in this Letter are obtained using distilled water at 25 °C (density $\rho = 997$ kg · m^{-3} and viscosity $\eta = 0.89$ mPa·s), an opening radius $r_0 = 1.75$ mm ($2r_0 \approx \kappa^{-1}$), and initial heights h_0 varying from 4 to 11 cm. With these experimental parameters, one can

TABLE I. Static contact angle θ_s (°) measured for water droplets for the different materials used as the tank bottom plate.

Glass	Dural	Plexiglas	PVC	H-glass	Teflon
13.2 ± 1.5	51.8 ± 1.6	63.8 ± 1.9	67.7 ± 1.3	87.7 ± 5.3	98.5 ± 3

estimate the values of the Reynolds numbers at the onset of the flows: $\mathrm{Re} \approx v_T(0) r_0 \eta/\rho$. They are found between 900 and 2500, thus in the ideal-fluid flow regime.

The tank is filled with fluid up to h_0. The fluid is heated to 25 °C and left at rest for a few minutes. The experiments start at $t = 0$ when the hole is opened; both jet shape and drained mass are recorded according to time. The typical duration for the hole openings is between 20 and 50 ms. Wettability of the bottom plate is changed by using different materials: glass, Dural, Plexiglas, PVC (polyvinyl chloride), glass made hydrophobic (H-glass; coated glass with Rain-X® Original Glass Water Repellent) and Teflon. We characterize the wetting properties of these surfaces by their static contact angle for water droplets, θ_s (Table I).

Results.—Figure 1 shows measurements of the drained volume V versus time t for two different initial heights h_0 and three bottom plates having different wetting properties. Within the experimental error, the measurements are reproducible. For the same height and the same plate (same hole radius and wettability) all obtained flow volume curves are similar. For a square tank, Torricelli's model predicts that the drained volume as a function of time is given by

$$V(t) = \pi r_0^2 \sqrt{2gh_0}\, t - \frac{\pi^2 r_0^4}{2a^2} g t^2. \qquad (1)$$

The dashed curves in Fig. 1 correspond to this model. As expected the experimental curves are below those of Torricelli's model, nonetheless, they exhibit similar behaviors with t. We observe that for the various bottom plates the obtained experimental curves are all different, thereby suggesting that the flow rate depends on the wetting. The fastest flow is seen for the glass plate, the slowest for the Plexiglas plate—i.e., for $\theta_s \approx 60°$—and the flow for the coated glass plate is in between both. Surprisingly, the slowest flows are obtained for a contact angle θ_s on the order of 60°, likely indicating a nonmonotonic effect of wetting. Experimental curves are fitted to a quadratic model $\alpha t^2 + \beta t$, where α and β are free parameters. This allows us to define both an effective radius r_0^{eff} and an initial height h_0^{eff} that are calculated from Eq. (1) using the fitting values of α and β. It should be noted that r_0^{eff} and h_0^{eff} are the values that the hole radius and the initial height of the fluid should be to obtain the experimentally measured flow if the fluid was flowing out at the velocity $\sqrt{2gh(t)}$. It is also worth mentioning that under certain initial conditions, jet instabilities occur at the flow start. These instabilities strongly depend on wetting and will not be described here. They last for a few seconds at the beginning of the experiment; however, this does not affect the shape of the measured drained volume curves that always fit to a parabola.

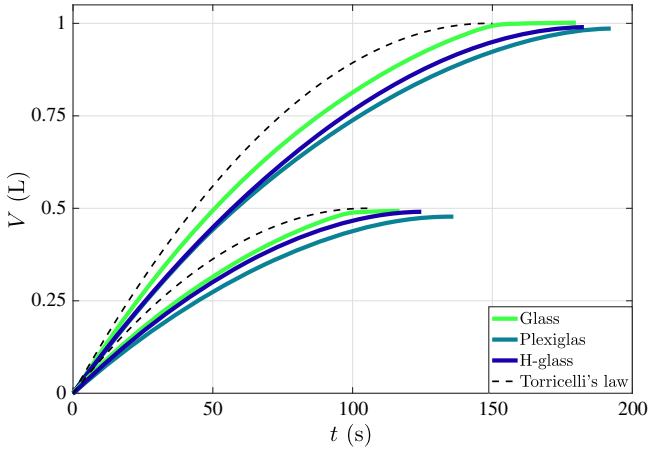

FIG. 1. Drained volume V versus t for $h_0 = 10$ cm (1 L) and 5 cm (0.5 L) [$r_0 = 1.75$ mm]. The different colors represent the different bottom plates, from dark, the more hydrophobic (coated glass) to light, the more hydrophilic (glass). Dashed curves correspond to the Torricelli's model. The line thickness is larger than uncertainties on the measured drained volumes.

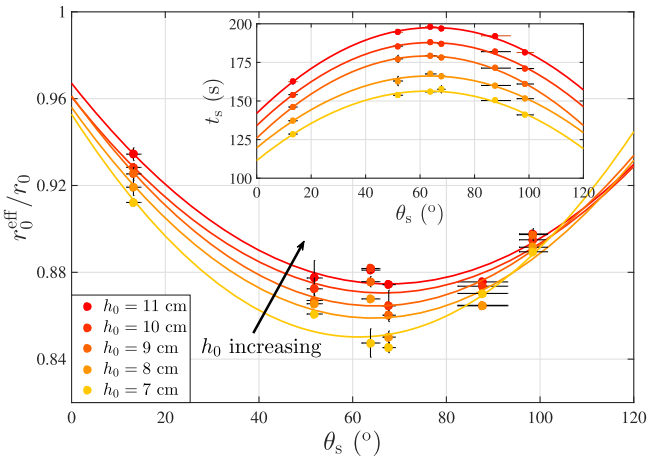

FIG. 2. r_0^{eff}/r_0 and t_s (inset) as a function of θ_s for different initial heights [$r_0 = 1.75$ mm]; r_0^{eff}/r_0 exhibits a minimum for $\theta_s \approx 60°$ where t_s shows a maximum. Lines are fits of r_0^{eff}/r_0 and t_s data to quadratic polynomial functions to point out their nonmonotonic evolution.

The normalized effective initial height h_0^{eff}/h_0 does not seem to depend on wetting. All obtained values of h_0^{eff}/h_0 are close to 1 (not shown), in the range [0.95–1.02], without regularity; thus $h_0^{\text{eff}} \approx h_0$. The normalized effective radius r_0^{eff}/r_0 is displayed depending on the wetting angle θ_s in Fig. 2. r_0^{eff} is always smaller than the opening radius and evolves with θ_s. Therefore all dissipation and wetting effects can be included in a single parameter r_0^{eff} in Eq. (1). Note that r_0^{eff} is not equal to the jet radius. For each θ_s, r_0^{eff} decreases with h_0. For each h_0, r_0^{eff} changes nonmonotonically with θ_s and shows a minimum for $\theta_s \approx 60°$, as expected from the drained volume curves. Another parameter that can be considered is the time t_s, which is defined as the moment when a discontinuity appears in the variation of $V(t)$. Looking at the jet, t_s is the moment when the jet starts to taper significantly just before drainage stops. It corresponds roughly to the duration required to drain the tank. t_s versus θ_s is shown in the Fig. 2 inset. For a given θ_s, t_s increases with h_0 as $\sqrt{h_0}$ and corresponds well to the end time of the flow that is predicted from Torricelli's model using r_0^{eff}; $t_s \approx (a^2\sqrt{2h_0/g})/\pi(r_0^{\text{eff}})^2$. t_s evolves with θ_s nonmonotonically and exhibits a maximum for $\theta_s \approx 60°$, in agreement with the variations of r_0^{eff}.

Further experiments were performed using as bottom plate a glass plate with only one of its sides hydrophobic (Supplemental Material [17], Appendix B). The hydrophobic side was set inside and outside the tank alternately to investigate different configurations. On the basis of these results, we assume that dissipation, both inside the tank and the orifice, does not depend on the wettability of the inner surface of the bottom plate and therefore the wettability effect on flow is only due to the wetting of the outer surface of the bottom plate with water. For given r_0 and h_0, without taking into account the instabilities that can be seen at the onset of the flow, the only difference between the flow jets from the different materials is the meniscus that forms at the hole's outlet (see Fig. 3). The shape of this meniscus evolves continuously with wettability; its lateral extension on the plate $r_{\text{jet}}(z=0)$ increases with the plate hydrophilicity (i.e., as θ_s decreases). We assume that the meniscus shape does not affect dissipation inside the tank. Hence we believe that the meniscus accelerates or decelerates the speed of drainage depending upon its shape and that therefore the explanation of the nonmonotonic effect of wetting on Torricelli's law is related to the meniscus shape. Thereby in an attempt to understand the effect of the meniscus shape on the flow, in others words the effect of θ_s, we propose a simple model that calculates the variation of the kinetic energy E_k due to a flow within the meniscus.

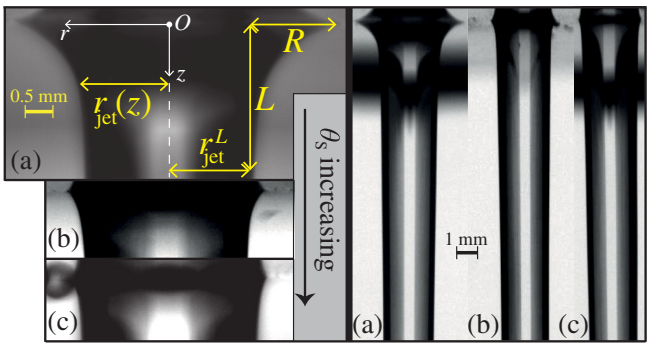

FIG. 3. Jets at the exit of the tank for similar conditions except wetting [$r = 1.75$ mm, $h_0 = 10$ cm and $t = 90$ s]. From hydrophilic to hydrophobic plate: (a) Glass ($\theta_s \approx 13°$), (b) Plexiglas ($\theta_s \approx 64°$), (c) H-glass ($\theta_s \approx 88°$). Left side: Zoom in of the jets at the hole exit to display the meniscus profiles for the different wetting conditions. Right side: Images of the jets to show their global shape; ≈5–6 mm beneath the opening exit the three jets look similar. The main notations of the model are reported in Fig. 3(a).

Modeling.—For all materials, even Teflon, a thin ring of fluid close to the wall, right at the exit of the hole, spreads outwards, radially and perpendicularly to the main flow, to wet the surface around the opening. This is the origin of the meniscus formation. Dissipation due to the radial flow at the plate level is neglected and this thin layer of fluid is not taken into account in the following. The meniscus always has a cylindrical symmetry and its outer shape follows a parabolic profile $r_{\text{jet}}(z)$ that goes from $r_{\text{jet}}(0)$ at the plate level ($r_{\text{jet}}(0) = r_{\text{jet}}^L + R$) to $r_{\text{jet}}(L) = r_{\text{jet}}^L$ at the point where the meniscus vanishes and connects to the jet [at $z = L$, $\partial_z(r_{\text{jet}}(L)) = 0$]. Note that r_{jet}^L is the jet radius right below the meniscus, it is not equal to r_0 nor r_0^{eff} and it can be larger than both. The meniscus profile can be expressed in terms of the distance from the plate z as follows: $r_{\text{jet}}(z) = (R/L^2)z^2 - (2R/L)z + R + r_{\text{jet}}^L$.

In this model, the meniscus is considered made of two distinct parts in which the flow is different. A cylindrical tube having a radius r_{jet}^L wherein a plug flow along the z axis and of speed $v_0(t)$ is assumed. $v_0(t)$ is defined as $v_0(t) = Q_v(t)/\pi(r_{\text{jet}}^L)^2$, where $Q_v(t)$ is the experimentally measured flow rate. Here, we neglect the fluid acceleration due to gravity over the meniscus length (i.e., $v_0 - v(L) = \sqrt{2gL} \ll v_0$). A junction of length L connects this tube to the bottom plate. Because of the radial symmetry, within this junction $v_\phi = 0$, and the velocity vector simply writes $\mathbf{v} = v_r\mathbf{e_r} + v_z\mathbf{e_z}$. In first order, the vertical fluid velocity v_z is assumed to follow a linear law with r. It should be noted that a parabolic profile was also tested without major changes. To avoid speed discontinuity at $r_{\text{jet}}(L)$, velocity at the edge of the junction $v_z(r_{\text{jet}}(z))$ is also assumed to vary linearly with z, from 0 at the plate level to v_0 at $z = L$. Using these assumptions, the vertical velocity profile v_z is expressed depending upon both z and r, the distance from the center of the jet as

$$r \le r_{\text{jet}}^L \quad v_z(r,z) = v_0 \tag{2}$$

$$r > r_{\text{jet}}^L \quad v_z(r,z) = \frac{v_0[r_{\text{jet}}(z) - r + z(r - r_{\text{jet}}^L)/L]}{r_{\text{jet}}(z) - r_{\text{jet}}^L}. \tag{3}$$

The fluid incompressibility equation together with the condition $v_r(r_{\text{jet}}^L) = 0$, gives the expression of v_r (for $r \ge r_{\text{jet}}^L$)

$$v_r(r,z) = \frac{Lrv_0}{R(L-z)^2}\left(\frac{r}{3} - \frac{r_{\text{jet}}^L}{2}\right) + \frac{Lv_0 {r_{\text{jet}}^L}^3}{6Rr(L-z)^2}. \tag{4}$$

Thanks to these profiles one can develop a hydrodynamic model of the meniscus by writing the Navier-Stokes equation (Supplemental Material [17], Appendix C). By multiplying the Navier-Stokes equation by $\mathbf{v}$, one finds out the equation for the instantaneous change in the volume kinetic energy density $\partial_t e_k = \rho \mathbf{v} \partial_t \mathbf{v}$. The instantaneous variation of kinetic energy within the meniscus dE_k/dt is obtained by integration of $\partial_t e_k$ over the meniscus volume Ω.

$$\frac{dE_k}{dt} \approx \int_\Omega \Big[-\rho(v_r v_z \partial_r v_z + v_z^2 \partial_z v_z) - v_z \partial_z P(z) + \eta v_z\left(\frac{\partial_r v_z}{r} + \partial_r^2 v_z + \partial_z^2 v_z\right) + \rho g v_z\Big] d\Omega \tag{5}$$

where η is the dynamical viscosity and $P(z)$ the local pressure. It is assumed that the pressure only depends on z and due to the junction shape, in addition to the atmospheric pressure P_0, Laplace's pressure within the meniscus must be taken into account. Thus $P(z)$ is written as $P(z) = P_0 + \gamma[1/r_{\text{jet}}(z) - 1/R_c(z)]$, where R_c is the curvature radius of the junction given by $R_c(z) = (1 + [\partial_z r_{\text{jet}}(z)]^2)^{3/2}/(\partial_z^2 r_{\text{jet}}(z))$.

Experimentally we observe that r_{jet}^L, R, and L depend on both the outer plate wettability θ_s as well as the time t through Q_v (R increases as v_0 diminishes, while r_{jet}^L decreases). Unfortunately, we do not have any analytical relationship between r_{jet}^L, R, L, θ_s and Q_v and therefore we are not able to predict $r_{\text{jet}}(z)$ as a function of the surface wettability and the flow rate. Consequently, we are not able to find out an expression of dE_k/dt solely as a function of θ_s and t. Thus, in order to compare our model with the experimental results, we calculate values of dE_k/dt at different flow rates Q_v for each wettability condition.

According to Eq. (5), four sources of variation are distinguished: nonlinear convection, local pressure, viscous dissipation, and hydrostatic pressure. The contribution of each term as a function of v_0, L, R, and r_{jet}^L can be calculated separately using the formal calculus software Mathematica. This provides an estimate of the respective weight of each term. In this framework the viscous dissipation is always negligible. From the experiments $v_0(Q_v)$, $R(Q_v)$, $L(Q_v)$, and $r_{\text{jet}}^L(Q_v)$ are obtained (Supplemental Material [17], Appendix D). Using these experimental values and the analytical expressions that are found for the four terms, $dE_k(Q_v)/dt$ are calculated for any Q_v. Figure 4 displays calculated values of dE_k/dt as a function of θ_s for $Q_v = 3$, 4 and 5 mL.s^{-1}, respectively. Although values of dE_k/dt calculated in this way are not very accurate for large values of θ_s (then R and L are rather difficult to estimate), one can notice that dE_k/dt is always positive. Thus whatever its shape, the meniscus always accelerates the flow with respect to a straight jet that would be without a meniscus at the hole's outlet. It also exhibits a minimum around $\theta_s \approx 60°$. Accordingly, t_s should have a maximum for $\theta_s \approx 60°$. This behavior can be understood as follows. For hydrophilic surfaces, R is on the order of a few millimeters and $L/R \approx 1$, then contributions of all terms in Eq. (5) are important, the largest one being that of the nonlinear convection term; accordingly dE_k/dt is high. As the surface hydrophobicity increases, R decreases while L/R grows up to 4–5, then contributions of all terms in Eq. (5) decline sharply, thus resulting in small values of dE_k/dt. For hydrophobic surfaces, meniscuses are small, R is on the order of hundreds of microns and $L/R \approx 2$, because of that the contribution of the local pressure term becomes very high, yielding large values of dE_k/dt (Supplemental Material [17], Appendix E). Nevertheless, the fluid never flows out quicker than what is predicted by Torricelli's model, because in the latter dissipation is neglected.

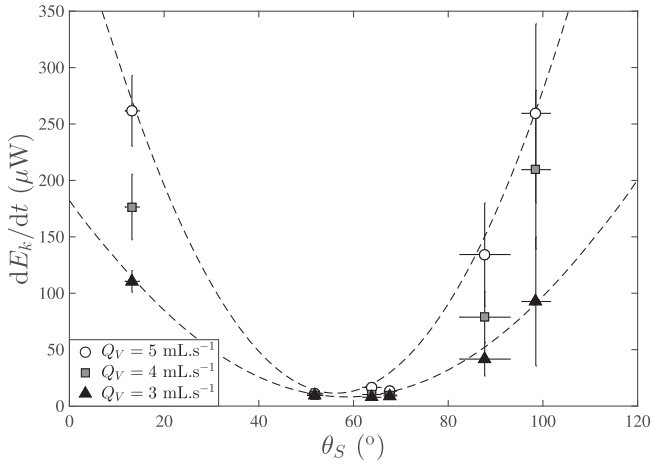

FIG. 4. Calculated values of dE_k/dt from Eq. (5) as a function of θ_s, for $Q_v = 3$, 4 and 5 mL.s^{-1}. Each value of dE_k/dt reported here is the average over several dE_k/dt values calculated at the same Q_v but for different h_0. The lines are guidelines to show the minimum.

Summary.—This work reports the effect of wetting on the draining of a tank through a hole of millimetric size, on the order of the fluid capillary length. The experimental results show that although the flow still follows behavior

that can be deduced from Torricelli's law, wetting strongly affects the speed of drainage that goes through a minimum as the outside surface of the tank bottom plate changes from hydrophilic to hydrophobic. The wetting seems to have a maximum effect in slowing down the flow for a static wetting angle θ_s of about 60°. Similar results were also obtained for other hole radii—smaller or on the order of magnitude of the capillary length κ^{-1}, i.e., within the range 0.5–2.5 mm. We propose that the nonmonotonic effect of wetting lies in the meniscus that forms at the hole outlet. A simple model that calculates the variation of kinetic energy within the meniscus captures the key points of this phenomenon. These few results are in agreement with the results presented here. We believe that this effect deserves further investigation, both theoretical and experimental, in particular to test other materials—like superhydrophobic surfaces—or other fluids.

*eric.freyssingeas@ens-lyon.fr

[1] E. Torricelli, Opera Geometrica, *De sphaera et Solidis Sphaeralibus; De Motu Gravium; De Dimensione Parabolae* (Amadoro Massa & Lorenzo de Landis, Florence, 1644).

[2] R. Ouziaux and J. Perrier, Mécanique des fluides appliquée—Tome 1—Fluides incompressibles, Dunod, Paris (1972).

[3] J. Boussinesq, Essai sur la théorie de l'écoulement d'un liquide par un orifice en mince paroi, C. R. Académie des Sciences, **114**, 704 (1870).

[4] H. von Helmholtz, Monatsber. Dtsch. Akad. Wiss. Berlin **1868**, 215 (1868).

[5] G. Kirchhoff, *Vorlesungen ber Matematische Physik, Forchheimer Hydrauli* (B. G. Teubner, Leipzig, 1876), p. 341.

[6] G. F. Davidson, Experiments on the flow of viscous fluids through orifices, Proc. R. Soc. A **89**, 91 (1913).

[7] C. Clanet, Clepsydrae, from Galilei to Torricelli, Phys. Fluids **12**, 2743 (2000).

[8] M. E. Saleta, D. Tobia, and S. Gil, Experimental study of Bernoullis equation with losses, Am. J. Phys. **73**, 598 (2005).

[9] T. Massalha and R. M. Digilov, Experimental evidence of capillary interruption of a liquid jet, Open Journal of Applied Sciences, **4**, 392 (2014).

[10] P. G. De Gennes, Wetting: statics and dynamics, Rev. Mod. Phys. **57**, 827, Part I (1985).

[11] D. Bonn, J. Eggers, J. Indekeu, J. Meunier, and E. Rolley, Wetting and spreading, Rev. Mod. Phys. **81**, 739 (2009).

[12] T. Blake and K. Ruschak, A maximum speed of wetting, Nature (London) **282**, 489 (1979).

[13] S. F. Kistler and L. E. Scriven, in *Computational Analysis of Polymer Processing, Coating Flows*, edited by J. R. A. Pearson and S. M. Richardson (Applied Science Publishers, London and New-York, 1983), Chap, 8, pp. 243–299.

[14] S. F. Kistler and L. E. Scriven, The teapot effect: sheet-forming flows with deflection, wetting and hysteresis, J. Fluid Mech. **263**, 19 (1994).

[15] C. Duez, C. Ybert, C. Clanet, and L. Bocquet, Making a splash with water repellency, Nat. Phys. **3**, 180 (2007).

[16] C. Duez, C.Ybert, C. Clanet, and L. Bocquet, Wetting Controls Separation of Inertial Flows from Solid Surfaces, Phys. Rev. Lett. **104**, 084503 (2010).

[17] See Supplemental Material at http://link.aps.org/supplemental/10.1103/PhysRevLett.117.248002 for Appendix A—details on the experiments. Appendix B—displays a set of experiments, which prove that the effect we report in the Letter is only due to the wetting of the outer surface of the bottom plate with water. Appendix C—details on the model and calculated expression of the different terms. Appendix D—details on how we compare the model with the experimental results. Appendix E—more details on the nonmonotonic evolution of dE_k/dt with θ_s.